Journal of Medical Ultrasound (2014) 22, 99—105

Available online at www.sciencedirect.com

ScienceDirect

journal homepage: www.jmu-online.com

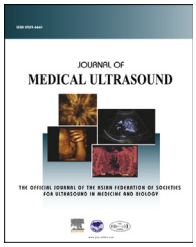

BRIEF COMMUNICATION

High-intensity Focused Ultrasound Ablation of Soft-tissue Tumors and Assessment of Treatment Response with Multiparametric Magnetic Resonance Imaging: Preliminary Study Using Rabbit VX2 Tumor Model

Kyung Won Kim [1,2,3], Jae Young Lee [1,2*], Jeong Min Lee [1,2], Yong Sik Jeon [1,2], Yoon Seok Choi [1,2], Jisuk Park [1,2], Harry Kim [1,2], Joon Koo Han [1,2], Byung Ihn Choi [1,2]

[1] *Department of Radiology,* [2] *Institute of Radiation Medicine, Seoul National University College of Medicine, and* [3] *Department of Radiology, Asan Medical Center, University of Ulsan College of Medicine, Seoul, South Korea*

Received 9 January 2013; accepted 29 January 2014
Available online 1 May 2014

KEY WORDS
diffusion-weighted images,
dynamic contrast-enhanced magnetic resonance imaging,
high-intensity focused ultrasound,
soft-tissue tumor

Background: High-intensity focused ultrasound (HIFU) is an emerging technique for noninvasive ablative treatment. However, HIFU has rarely been performed for the treatment of soft-tissue tumors. Thus, we aimed to assess the feasibility and safety of performing extracorporeal HIFU for the treatment of soft-tissue tumor. The treatment response was assessed using functional magnetic resonance imaging (MRI) techniques.
Materials and methods: In the rabbit VX2 intramuscular tumor model, HIFU was performed using an extracorporeal HIFU device (YDME FEP-BY02) by varying the electric power from 50 to 400 W, with the other parameters being fixed. The HIFU beam was insonated to one layer of focal spots having a depth of 8 mm. The degree of ablation was evaluated by histological examination and functional MRI techniques including dynamic contrast-enhanced MRI (DCE-MRI) and apparent diffusion coefficient (ADC) map. The presence of skin burn was also evaluated.
Results: Applying HIFU with an electric power of 200 W discretely produced the ablation zone without skin burn as planned before treatment (maximal depth: 8—9 mm), which shows the suitability of using HIFU (with 200 W electric power) for the treatment of soft-tissue tumors.

Conflicts of interest: All contributing authors declare no conflicts of interest.

* Correspondence to: Dr Jae Young Lee, Department of Radiology, Seoul National University College of Medicine, 28 Yeongon-dong, Jongno-gu, Seoul 110-744, Korea; Institute of Radiation Medicine, Seoul National University College of Medicine, 28 Yeongon-dong, Jongno-gu, Seoul 110-744, South Korea.
E-mail address: leejy4u@snu.ac.kr (J.Y. Lee).

http://dx.doi.org/10.1016/j.jmu.2014.02.006

By contrast, HIFU with an electric power of 100 W produced an ill-marginated ablation zone with internal residual tumor foci, and HIFU with 300—400 W produced ablation zones with a maximum depth of 13—24 mm, which far exceeded the planned depth and caused skin burn. Perfusion maps of DCE-MRI demonstrated the devascularized ablation zone more conspicuously than conventional contrast-enhanced T1-weighted images, and ADC map demonstrated the surrounding edema or granulation tissue better than conventional T2-weighted images.
Conclusion: Extracorporeal HIFU treatment for soft-tissue tumor may be a feasible approach with adjustment of input energy level. For post-treatment assessment, functional MRI techniques including DCE-MRI and ADC map may be useful and complementary to conventional MRI.

Introduction

High-intensity focused ultrasound (HIFU) is an emerging ultrasound technique for noninvasive ablative treatment [1]. Despite the expanding use of HIFU for the treatment of various tumors, only a few studies were conducted on the application of HIFU for soft-tissue tumors or intramuscular tumors [2,3]. Soft-tissue tumors develop in the connective tissues other than the bone, such as the skeletal muscle, fat, fibrous tissue, or neurovascular tissue. Although soft-tissue tumors can occur anywhere in the body, they are most frequent in the extremities. At present, the standard treatment of soft-tissue tumors in the extremities consists of limb-sparing surgery and adjuvant radiation and/or chemotherapy. However, in case of small soft-tissue tumors, HIFU may be used as an alternative treatment, because therapeutic ultrasound energy can penetrate soft tissue with a relatively good sonic window compared with that of deep-seated organs such as the liver or pancreas.

Determination of optimal *in situ* acoustic energy is crucial to achieve focused complete ablation as well as to avoid complications such as unnecessary extensive ablation of adjacent soft tissue or major skin burns, which might be prevented by adjusting HIFU treatment parameters. Thus, we aimed to assess the feasibility and safety of HIFU treatment using an extracorporeal HIFU device (YDME FEP-BY02; Yuande Biomedical Engineering, Beijing, China) for the treatment of soft-tissue tumor in a preclinical rabbit model. Because ultrasound monitoring has limitations for accurate assessment of treatment response after ablation [4], multiparametric magnetic resonance imaging (MRI) including dynamic contrast-enhanced MRI (DCE-MRI) and its perfusion maps, diffusion-weighted images (DWIs), and an apparent diffusion coefficient (ADC) map were evaluated for treatment monitoring after HIFU.

Materials and methods

Animal model

The intramuscular VX2 tumor model in rabbits was used in this study. The VX2 tumor is a papilloma virus-induced tumor of epithelial origin and permits allogenic transplantation [5]. Ten adult New Zealand white rabbits, each weighing 3.0—3.5 kg, were used in this study. The VX2 tumor strain was maintained by successive transplantations of tumor cells into the hind limbs of the carrier rabbits. Anesthesia was induced by administering an intravenous injection of ketamine hydrochloride (50 mg/kg body weight; Ketamine, Yuhan, Korea) and 2% xylazine (0.1 mL/kg; Rompun, Bayer, Germany). After shaving the paravertebral area, 0.15 mL of minced tumor was implanted using an 18-gauge MEDICUT needle in the paravertebral muscles symmetrically at both sides. An animal model containing a superficially located intramuscular tumor was prepared to evaluate both treatment efficacy and safety (i.e., skin burn) of the HIFU treatment. Thus, we used ultrasonography for guiding the MEDICUT needle 1 cm below the skin surface. This method allowed the growth of a single, solitary, well-demarcated tumor in the superficial layer of the paravertebral muscles of each recipient rabbit. Two weeks following the tumor implantation and approximately when the tumors were expected to be round in shape with a 1.5—2.0 cm diameter, HIFU was performed. Among the 10 rabbits, one showed no tumor. Therefore, the remaining nine rabbits underwent HIFU. The maximum diameter of all 16 tumors, as seen on axial contrast MR images, ranged from 1.4 to 2.2 cm (mean: 1.6 $\pm$ 0.5 cm).

HIFU treatment

The FEP-BY02 HIFU system (Yuande Biomedical Engineering Limited Corporation, Beijing, China) was used in our experiments. The therapeutic HIFU transducer was a fixed focus concave transducer, which contained 251 piezoelectric elements with an overall aperture of 37 cm and a focal length of 26 cm. The elements of the therapeutic transducer are driven in phase at a frequency of 1.04 MHz. The focal zone of the therapeutic transducer was an elongated ellipsoid with an axial length of 8 mm (−6 dB) and radial diameter of 3 mm. The diagnostic ultrasound system (GE LOGIQ 5; GE Healthcare, Seongnam, Korea) with a 5-MHz linear probe was mounted coaxially to the HIFU therapeutic transducer. The tumors were imaged with the diagnostic imaging transducer and positioned in the center of the focal zone of the therapeutic transducer. The treatment area and number of spots were then determined. The HIFU beam was insonated into the tumor and moved successively through each spot.

To identify the degree of ablation according to the energy delivered by the HIFU source, the electric power

delivered to the HIFU transducer was varied from 50 to 400 W, while fixing the other parameters. Other treatment parameters that this HIFU system allows the operator to specify were set as follows: pulse length, 150 ms; intermission time between pulses, 150 ms; duty factor, 0.5; number of pulses per spot, 70; interval spacing between spots, 3 mm; and the distance between the skin surface and the HIFU focus, 5 mm. In this study, we applied HIFU treatment to only one layer of focal spots, which has a depth of 8 mm, even though the tumor depth exceeded 8 mm. We divided the rabbits into five groups and performed HIFU to each group with different energy levels. The treatment parameters are summarized in Table 1. Depending on the tumor size, treatment duration varied from 16 to 18 minutes. The HIFU technique was applied to a tumor on one side of the paravertebral muscles, while the tumor on the other side of the paravertebral muscles was used as the control.

Multiparametric MRI acquisition

To evaluate the HIFU treatment response, MR imaging studies were performed on Day 1 and Day 5 post-HIFU treatment. All MR examinations were performed on a 3-Tesla MR system (TIM Trio; Siemens Medical Systems, Erlangen, Germany) with a standard eight-channel knee coil. First, unenhanced T2-weighted images (T2-WIs) were obtained with the following parameters: repetition time/echo time (TR/TE), 4100/87 ms; matrix size, 128 × 128; slice thickness, 3 mm; and field of view (FOV), 130 × 130 mm. Second, unenhanced T1-weighted images (T1-WIs) were acquired at each of the two flip angles for T1 mapping using the following parameters: TR/TE, 4.4/1.1 ms; flip angles (α) = 2° and 15°; matrix size, 128 × 128; slice thickness, 3 mm; number of slices, 20; and FOV, 140 mm. DCE-MRI using the T1-weighted radial gradient echo sequence was then performed with an intravenous bolus injection of 0.1 mmol/kg of gadopentetate dimeglumine (MAGNEVIST; Bayer Schering, Seoul, Korea). The parameters used were as follows: TR/TE, 3.5/1.5 ms; flip angle (α) = 11°; matrix size, 128 × 128; slice thickness, 3 mm; number of slices, 20; and FOV, 140 mm. In this study, a hybrid three-dimensional stack-of-stars trajectory was used. The DCE-MRI was continuously scanned 20 times during 240 seconds. We used K-space-weighted image contrast (KWIC) reconstruction technique to obtain high temporal resolution, while maintaining high spatial resolution [6]. With KWIC technique, four time-resolved subframe images were reconstructed from one scan, enabling a 3-second temporal resolution in our study (240 seconds/20 scans × 4 subframe images). Using the subframe, DCE-MRI images, voxelwise perfusion maps of the volume transfer coefficient (K-trans) were generated with a postprocessing software program (Tissue 4D; Siemens AG, Erlangen, Germany), which is based on the Tofts model [7,8]. The DWI used a spin-echo echo-planar imaging sequence (TR/TE = 3800/69 ms) with diffusion gradients applied in the x, y, and z axes (b = 500 mm/s^2). The FOV was 130 × 130 mm and the matrix size was 64 × 64. The ADC values were measured for each of the three directions (x, y, and z) and averaged for the calculation of the final ADC value.

Gross examination and histology

The presence of skin burns was evaluated immediately after ablation. At 5 days after ablation, the rabbits were killed and frozen in a refrigerator at −70 °C. Two days later, each frozen rabbit was cut in a transverse plane using a power saw, and gross specimens were sliced transversely at 5-mm intervals to match the MR images. The tissue was processed by standard histopathological techniques and stained with hematoxylin and eosin (H&E).

Results

Therapeutic effects according to the HIFU energy level

The depth of the ablation zone became larger as the energy of the HIFU beam increased (Table 1). In Group 1, which was treated with the lowest HIFU power (50 W), the tumor was not ablated at all, shown as contrast-enhancing mass on MRI. When treating the tumors with an electric power of 100 W (Group 2) and 200 W (Group 3), the maximal depth of the ablation zone measured on MRI reached 8–9 mm, which was similar to the depth of focal spots (8 mm) as planned before treatment. When we applied high input electric power (300 W in Group 4 and 400 W in Group 5), the depth of the ablation zone far exceeded the planned depth along the beam axis (13–15 mm in Group 4 and 24 mm in Group 5). The ablated zones of Groups 3–5 were discretely produced (Fig. 1), while those of the Group 2 were less clearly marginated with some residual viable tumor foci in the ablation zone in the H&E histological section (Fig. 2).

Table 1 Treatment parameters and results of high-intensity focused ultrasound treatment.

Groups	Power (W)	Acoustic intensity (ISATA, W/cm^2)	Acoustic energy (J)	Maximum depth of ablation zone (mm)[a]	Skin burn[a]	Survival[a]
1	50	388	263	0/NA[b]	−	+
2	100	776	526	8/8	−/−	+/+
3	200	1552	1052	8/9	−/−	+/+
4	300	2328	1578	13/15	+/+	+/Died (5 days)
5	400	3104	2104	24/NA[c]	+/++	+/Died (3 hours)

[a] Results of the first rabbit/second rabbit in each group.
[b] Not available because the tumor was not grown in this rabbit.
[c] Not available because the rabbit died 3 hours after ablation, before undergoing magnetic resonance imaging.

Regarding the safety of the HIFU treatment, rabbits treated with low energy level (Groups 1—3) tolerated the HIFU treatment without significant event and showed normal activity during 5 days of follow up after the treatment (Table 1). One rabbit in Group 4 lost weight from 2.9 to 2.6 kg and died at 5 days after ablation. One rabbit in Group 5 died 3 hours after the HIFU therapy, probably due to major burn injuries and/or anesthesia. *Post mortem* MRI and autopsy were not performed. Skin burn occurred only in rabbits of Groups 4 and 5. These results support that the energy level used in Group 3 (power 200 W, ISATA 1552 W/cm^2, and acoustic energy 1052 J/spot) can be recommended for HIFU treatment of the superficially located soft-tissue tumors.

Multiparametric MRI findings of the ablation zone

On the MRIs obtained on Day 1 and Day 5 after the treatment, the ablation zones were shown as devascularized areas without enhancement on contrast-enhanced T1-WI, while the remnant tumors were shown as contrast-enhancing lesions (Figs. 1 and 2). The K-trans perfusion map of DCE-MRI also demonstrated the ablation zones as devascularized areas with a very low K-trans value near zero (Fig. 1). The devascularized areas were more clearly depicted in the K-trans perfusion map than in conventional contrast-enhanced T1-WI. The T2-WI was not helpful to delineate the ablation zone. On T2-WI, the completely devascularized ablation zones were shown as hypointense

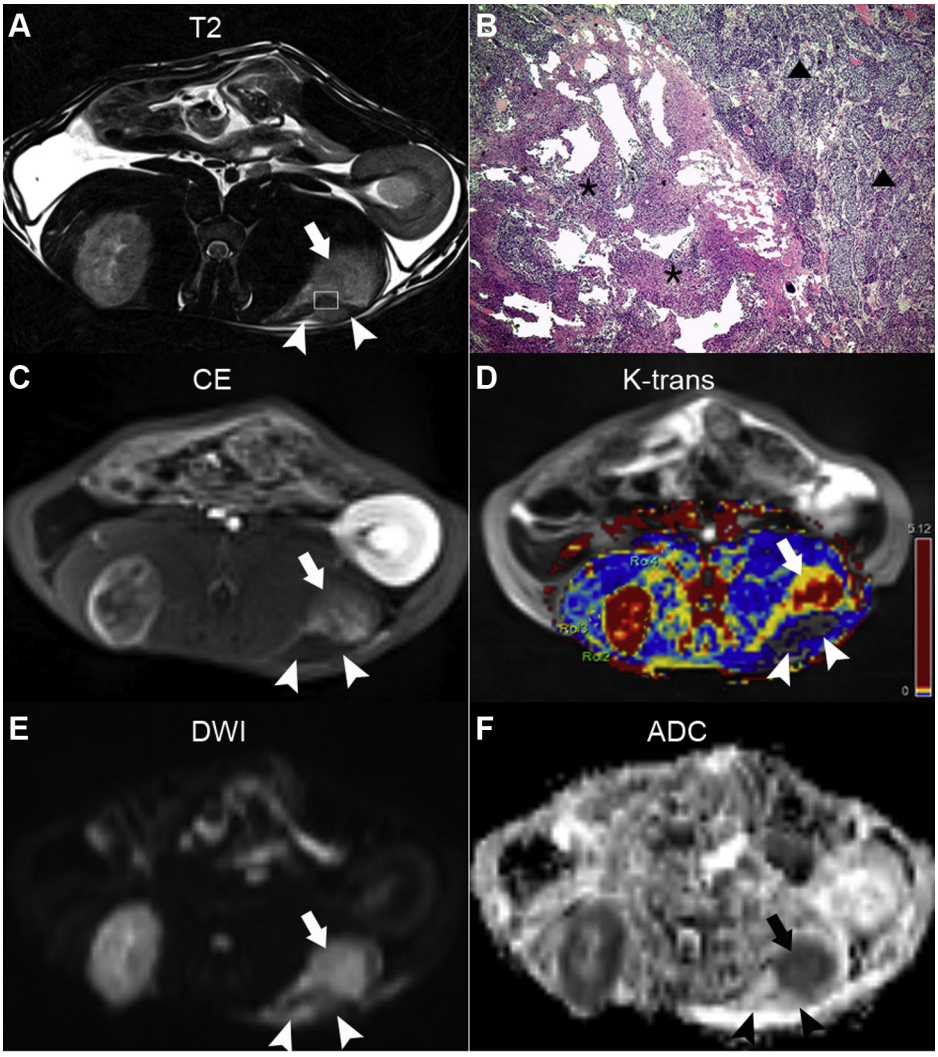

Fig. 1 Magnetic resonance imaging performed 5 days after high-intensity focused ultrasound ablation with an electric power of 200 W. (A) On the T2-weighted image (T2-WI), the hypointense band (arrowheads) of the ablation zone is clearly distinct from the residual tumor (arrow). The hyperintense area posterior to the hypointense band is also part of the ablation zone. (B) The hematoxylin and eosin (40×) histological specimen, which corresponds to the small box in (A) also shows a clear distinction between the ablation zone with coagulative necrosis (asterisks) and the viable residual tumor (triangles). (C) The ablation zone is shown as a devascularized area without any contrast enhancement (CE) on contrast-enhanced T1-weighted image (T1-WI) and (D) a gray-colored defect area on the K-trans color map overlapped on T1-WI. (E) The ablation zone shows low signal intensity (SI) on diffusion-weighted image (DWI) and (F) high apparent diffusion coefficient (ADC) value on ADC map, whereas the residual tumor shows high SI on (E) DWI and low ADC value on (F) ADC map.

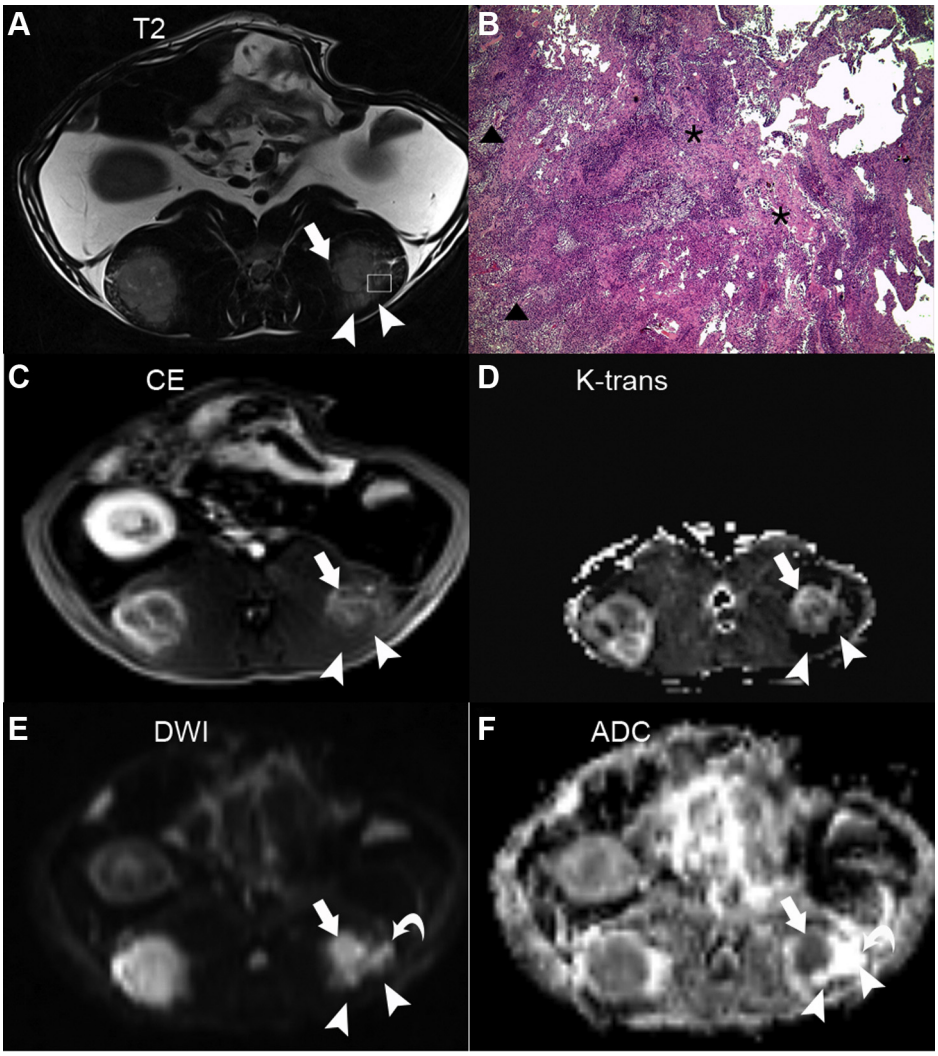

Fig. 2 Magnetic resonance imaging performed 1 day after high-intensity focused ultrasound ablation with an electric power of 100 W. (A) On the T2-weighted image (T2-WI), both the ablation zone (arrowheads) and residual tumor (arrow) show high signal intensity. (B) The hematoxylin and eosin (40×) histological section, which corresponds to the small box in (A) shows the indistinct margin between the area of coagulative necrosis (asterisks) and the viable residual tumor portion (triangles). (C) The ablation zone (arrowheads) is not clearly distinct from adjacent muscle tissue on contrast-enhanced (CE) T1-weighted image, whereas (D) it is well demonstrated as a devascularized area on the K-trans gray map. (E) On diffusion-weighted image (DWI), the residual tumor (arrow) is not distinct from the ablated zone (arrowheads) and adjacent edema (curved arrow) due to similar degree of hyperintensity. (F) However, apparent diffusion coefficient (ADC) map clearly shows the residual tumor due to its low ADC value, whereas the adjacent edema has a high ADC value.

lesions, while the surrounding edematous changes were manifested as ill-marginated hyperintense areas. Necrotic areas within the ablation zone were sometimes manifested as hyperintense areas. The border of remnant tumor and the edematous area were hardly differentiated on T2-WI and DWI due to their similar degree of high signal intensity. However, the ADC map enabled us to differentiate the remnant tumor from edema, as the tumor showed a low ADC value, whereas the edema had a high ADC value (Fig. 2). These MRI findings did not differ either in 1 day post-treatment MRIs and in 5 days post-treatment MRIs.

The H&E histological finding was correlated with contrast-enhanced MR findings. The areas of coagulation necrosis on histological specimen corresponded to the devascularized areas on MRI. In the ablated tumors with high energy level (Groups 3–5), the areas of coagulation necrosis were clearly distinguished from adjacent muscles or viable tumor portions on both histological specimen and contrast-enhanced MRI (Fig. 1B), whereas the tumors treated with low energy level (Group 2) showed indistinct margins between the ablated zones and the residual tumor portions in both MRI and histological specimen (Fig. 2).

Discussion

In this preclinical study to evaluate the feasibility and safety of HIFU using an extracorporeal system (YDME FEP-BY02) for the treatment of soft-tissue tumor, the area of the ablation zone was dependent on the energy delivered

by the HIFU source. The energy level for Group 3 (power, 200 W; ISATA, 1552 W/cm^2; and acoustic energy, 1052 J/spot) might be suitable for superficially located small soft-tissue tumors. Practically, the input power to HIFU device and the HIFU exposure time are the commonly used adjustable parameters for operators to set the HIFU protocol [9]. The *in situ* acoustic energy (E_A) was calculated based on the input electrical power (P_E), efficiency of the transducer (ε_T), estimation of tissue attenuation (α), and total time of HIFU exposure/spot calculated by multiplying the pulse length (τ_p), duty factor (df), and number of pulses per site [n_p; Eq. (1)] [10]. To achieve the desired *in situ* acoustic energy, the input electric power should be adjusted with respect to the estimated tissue attenuation, which was calculated based on the tumor depth and skin thickness. Because our experimental setting was used for a superficial intramuscular tumor model (distance from the skin surface to the HIFU focus: 5 mm), the input electric power should be increased for HIFU treatment of deeper lying tumors.

$$E_A = P_E \cdot \varepsilon_T \cdot 10_{10}^{-\alpha} \cdot [\tau_P \cdot df \cdot n_P] \quad (1)$$

In terms of HIFU exposure method and time, short pulses with a duty factor of 0.5 were used for the total exposure time of 10.5 seconds/spot considering the protocols of previous studies, which used this HIFU device [10–12]. It is well-known that different biological consequences result from different modes of ultrasound energy delivery. Continuous exposure to a HIFU beam causes rapid increase in tissue temperature to high degrees in a short period (a few seconds/spot) and results in thermal coagulation necrosis [9]. Short-pulsed HIFU exposure with low repetition rate (duty factor: 0.05–0.15) delivers the energy over a much longer time (few minutes/spot) and predominantly causes mechanical effects such as cavitation with mild hyperthermia. Therefore, it can be used to enhance the effect of concomitant chemotherapeutic drug or the delivery of the drug [13]. Although the continuous exposure provides uniform thermal ablation rapidly, thermal safety in surrounding tissues should be considered. A dose accumulation effect during periods of continuous exposure could lead to unwanted thermal lesions in surrounding tissues, especially along the beam axis (below and above the beam axis) [14]. The rationale for adopting short pulses with a duty factor of 0.5 (150 ms on and 150 ms off) in this study is that it can provide uniform thermal ablation of the target area while reducing the unwanted thermal effect to surrounding tissues by reducing the dose accumulation effect due to the cooling time between pulses.

Treatment assessment after HIFU ablation with short-term follow-up imaging is very important to guide the further treatment plan, which includes: (1) assessment of the ablation zone with differentiation of unablated residual tumor or adjacent muscle tissue; (2) characterization of reactive change in the ablated zone such as surrounding edema or granulation tissue; and (3) detection of treatment-associated complications such as hemorrhage or unexpected injury of adjacent organs. At present, MRI is the best modality for fulfilling these goals of treatment assessment after ablation [4].

Currently, contrast-enhanced T1-WI is known to be the most useful sequence in conventional MRI for the evaluation of ablated zone, which is shown as an unenhanced devascularized area and can be differentiated from enhancing residual tumor portion [4]. However, differentiation between the ablation zone and the adjacent non-ablated muscle tissue is sometimes difficult even on contrast-enhanced T1-WI, because normal muscle tissue may be barely enhanced on contrast-enhanced T1-WI. Perfusion map of the DCE-MRI may differentiate the ablation zone from the adjacent muscle tissue better than contrast-enhanced T1-WI, as shown in Fig. 2, because the perfusion map is highly sensitive to detect the perfusion change of the tissue. It coincides with a previous report about the perfusion map of the HIFU ablation zone of rabbit thigh muscle, which revealed that K-trans and Ve maps demonstrated the regions of histological change not visible on conventional MRI and were more accurately correlated with the histology [15].

Differentiating the residual tumor from the surrounding edema or granulation tissue on conventional MRI is frequently difficult, because the degree of T2 hyperintensity and contrast enhancement on T1-WI is similar in both granulation tissue and residual tumor. The ADC map is known to be helpful for differentiating the residual tumor from the surrounding edema or granulation tissue at the margin of the ablated zone, because the ADC value of residual tumor is lower than that of edema and granulation tissue, as shown in Figs. 1 and 2 [4]. Our results showed that the perfusion map of DCE-MRI and ADC map may be useful to evaluate the short-term response after HIFU treatment.

In conclusion, extracorporeal HIFU treatment for soft-tissue tumors appears to be feasible with adjustment of input energy level. For treatment assessment after HIFU treatment, functional MRI techniques including DCE-MRI and ADC map may be useful to provide additional information, which can complement conventional MRI sequences.

Acknowledgments

This work was partly supported by grants from the Korean Health and Medical Technology R&D Project, Ministry for Health, Welfare & Family Affairs (Grant No. A100265) and R&D program of Ministry of Knowledge Economy/Korea Evaluation Institute of Industrial Technology (Grant No. MKE/KEIT 10043474, Development of an Ultrasound Guided HIFU Treatment System).

References

[1] Kennedy JE. High-intensity focused ultrasound in the treatment of solid tumours. Nat Rev Cancer 2005;5:321–7.
[2] Wu F, Wang ZB, Chen WZ, et al. Extracorporeal high intensity focused ultrasound ablation in the treatment of 1038 patients with solid carcinomas in China: an overview. Ultrason Sonochem 2004;11:149–54.
[3] Wu F, Wang ZB, Chen WZ, et al. Extracorporeal focused ultrasound surgery for treatment of human solid carcinomas: early Chinese clinical experience. Ultrasound Med Biol 2004;30:245–60.
[4] Zhang Y, Zhao J, Guo D, et al. Evaluation of short-term response of high intensity focused ultrasound ablation for

primary hepatic carcinoma: utility of contrast-enhanced MRI and diffusion-weighted imaging. Eur J Radiol 2011;79:347—52.
[5] Kidd JG, Rous P. A transplantable rabbit carcinoma originating in a virus-induced papilloma and containing the virus in masked or altered form. J Exp Med 1940;71:813—38.
[6] Kim KW, Lee JM, Jeon YS, et al. Free-breathing dynamic contrast-enhanced MRI of the abdomen and chest using a radial gradient echo sequence with K-space weighted image contrast (KWIC). Eur Radiol 2013;23:1352—60.
[7] Tofts PS, Kermode AG. Measurement of the blood-brain barrier permeability and leakage space using dynamic MR imaging. 1. Fundamental concepts. Magn Reson Med 1991;17:357—67.
[8] Tofts PS, Brix G, Buckley DL, et al. Estimating kinetic parameters from dynamic contrast-enhanced T(1)-weighted MRI of a diffusable tracer: standardized quantities and symbols. J Magn Reson Imaging 1999;10:223—32.
[9] McDannold NJ, King RL, Jolesz FA, et al. Usefulness of MR imaging-derived thermometry and dosimetry in determining the threshold for tissue damage induced by thermal surgery in rabbits. Radiology 2000;216:517—23.
[10] Hwang JH, Wang YN, Warren C, et al. Preclinical *in vivo* evaluation of an extracorporeal HIFU device for ablation of pancreatic tumors. Ultrasound Med Biol 2009;35:967—75.
[11] Lee JY, Choi BI, Ryu JK, et al. Concurrent chemotherapy and pulsed high-intensity focused ultrasound therapy for the treatment of unresectable pancreatic cancer: initial experiences. Korean J Radiol 2011;12:176—86.
[12] Xiong LL, Hwang JH, Huang XB, et al. Early clinical experience using high intensity focused ultrasound for palliation of inoperable pancreatic cancer. JOP 2009;10:123—9.
[13] Hundt W, Yuh EL, Bednarski MD, et al. Gene expression profiles, histologic analysis, and imaging of squamous cell carcinoma model treated with focused ultrasound beams. AJR Am J Roentgenol 2007;189:726—36.
[14] Palussière J, Salomir R, Le Bail B, et al. Feasibility of MR-guided focused ultrasound with real-time temperature mapping and continuous sonication for ablation of VX2 carcinoma in rabbit thigh. Magn Reson Med 2003;49:89—98.
[15] Cheng HL, Purcell CM, Bilbao JM, et al. Prediction of subtle thermal histopathological change using a novel analysis of Gd-DTPA kinetics. J Magn Reson Imaging 2003;18:585—98.